



Missouri University of Science and Technology  
Scholars' Mine

---

International Specialty Conference on Cold-Formed Steel Structures

(1971) - 1st International Specialty Conference on Cold-Formed Steel Structures

---

Aug 20th, 12:00 AM

## Effects of Strain Hardening and Aging on Corner Properties of Cold-formed Steel Shapes

Kenneth W. Karren

M. M. Gohil

Follow this and additional works at: <https://scholarsmine.mst.edu/isccss>

 Part of the [Structural Engineering Commons](#)

---

### Recommended Citation

Karren, Kenneth W. and Gohil, M. M., "Effects of Strain Hardening and Aging on Corner Properties of Cold-formed Steel Shapes" (1971). *International Specialty Conference on Cold-Formed Steel Structures*. 1. <https://scholarsmine.mst.edu/isccss/1iccfss/1iccfss-session1/1>

This Article - Conference proceedings is brought to you for free and open access by Scholars' Mine. It has been accepted for inclusion in International Specialty Conference on Cold-Formed Steel Structures by an authorized administrator of Scholars' Mine. This work is protected by U. S. Copyright Law. Unauthorized use including reproduction for redistribution requires the permission of the copyright holder. For more information, please contact [scholarsmine@mst.edu](mailto:scholarsmine@mst.edu).

EFFECTS OF STRAIN HARDENING AND AGING ON  
CORNER PROPERTIES OF COLD-FORMED STEEL SHAPES

by

Kenneth W. Karren\*, M. ASCE and M. M. Gohil\*\*

SYNOPSIS

More economical design is possible in light-gage steel members if the increase in yield strength resulting from cold-forming is utilized. Such increases in yield strength are much larger in corner than in flat regions of cold-formed sections. A previous investigation<sup>1</sup> established an analytical method by which the increase in yield strengths could be predicted for corners in which a relatively large amount of plastic straining had occurred. In such corners with large plastic strain, it was found that the increase in strength could be attributed almost entirely to strain hardening. This study extends the method to apply to corners in which a relatively small amount of plastic straining has occurred. In these corners with small plastic strain the increase in yield strength can be attributed primarily to the phenomenon of strain aging.

INTRODUCTION

Some common cold-formed light-gage steel members are shown in Fig. 1. Large plastic strains occur in the corners of members such as the channel and angle sections. On the other hand, much smaller plastic strains occur in seamed welded tubing fabricated from sheet steel.<sup>2</sup> The geometry of a corner is similar to that of the tubing, i.e. corners are partial bodies of revolution and tubes are complete bodies of revolution. Hence, it seems logical to apply the methods already developed for cold-formed corners to cold-formed tubing.

A relation was derived in a previous investigation<sup>1</sup> relating the yield strength to the a/t (inside radius/thickness) ratio of corner specimens. The relation was shown to be valid for experimental results with a/t ratios varying from 1 to 7. The purpose of the investigation described herein<sup>4</sup> was to extend this work and experimentally check its validity for a/t ratios up to 100. This larger range includes the a/t ratios found in cold-formed welded steel tubing.

In an investigation of the fundamental strain hardening and strain aging behavior of several common types of mild steels, Chajes, Britvec, and Winter<sup>3</sup> found that the phenomenon of strain aging is more significant for small plastic strains than for large ones. The influence of strain aging is practically negligible for plastic strains larger than 0.10. Thus, it is likely that strain aging is of much more importance in the case of the large a/t ratios occurring in welded steel tubing than in the case of the small a/t ratios occurring in most cold-formed corners. To investigate this possibility, three types of tensile and compressive tests were conducted on a hot rolled light gage steel at Brigham Young University:

- (1) A series of cold-formed corners with a/t ratios varying from 1.4 to 70 were aged at room temperature for several months and tested.
- (2) Specimens were taken from the unworked flat material from which the corners were formed. Compressive specimens were tested to obtain the compressive yield strength.

Tensile specimens were tested in the plastic range to establish tensile yield strength, ultimate strength values, and values of the so-called strength coefficient k and strain hardening exponent n corresponding to the plastic stress-strain relationship

$$\bar{\sigma} = k(\bar{\epsilon})^n \quad (1)$$

These values (referred to herein as  $k_2$  and  $n_2$ ) were then used to predict corner yield strength values for the corners tested. (3) Additional tensile specimens of the flat sheet steel were prestrained to various amounts of tensile plastic strain and then artificially aged in an oven at 100°C for one half hour. The specimens were again tested to establish stress-strain characteristics in the plastic domain. The yield strengths from these tests were used in establishing new values of k and n, (referred to herein as  $k_3$  and  $n_3$ ). In this case n might well be called the strain hardening and strain aging exponent. This series of prestrained and aged specimens gave a reduced value for the exponent n, i.e.  $n_3 < n_2$ . For values of the a/t ratio larger than 10, it was found that the correlation between the theoretical and experimental corner yield strength values was considerably better for the prestrained, aged specimen  $k_3$  and  $n_3$  values than from the unrestrained specimen  $k_2$  and  $n_2$  values.

ANALYTICAL CORNER YIELD STRENGTH

For completeness, a brief description is included of fundamental concepts regarding (1) the role of true stress and true strain in inelastic stress strain relationships, (2) the strain hardening, and (3) the strain aging phenomena. These concepts will then be used in a brief recapitulation of the concepts used in obtaining the corner yield strength prediction equation developed in reference 1.

True Stress and Strain. True stress  $\sigma'$  is defined<sup>6</sup> to be

$$\sigma' = P/A \quad (2)$$

where A is the instantaneous area of a cross section corresponding to a given load P. In a ductile material true stress continues increasing up to the ultimate load while conventional stress decreases after the ultimate load is reached. Up to the point where a cross-section begins to neck down, true stress  $\sigma'$  may be related to engineering stress  $\sigma$  and engineering strain by the equation

$$\sigma' = \sigma(1+\epsilon) \quad (3)$$

True strain  $\epsilon'$  may be calculated from

$$\epsilon' = \ln(l/l_0) \quad (4)$$

where  $l$  is the instantaneous and  $l_0$  is the initial element length. True strain  $\epsilon'$  is related to engineering strain by the equation

$$\epsilon' = \ln(1+\epsilon) \quad (5)$$

True stress and strain are sometimes referred to as natural stress and strain.

\*Professor, Department of Civil Engineering, Brigham Young University, Provo, Utah.

\*\*Former graduate student, Department of Civil Engineering, Brigham Young University, Provo, Utah.

**Strain Hardening.** It is well known that mild steel exhibits stress-strain characteristics peculiar to most other types of metals, excluding certain types of brass, i.e., the stress-strain curve is characterized by (1) a straight line relationship in the elastic domain, (2) an upper yield point, (3) followed closely by a drop in load usually called the lower yield point, (4) a long stable yield plateau in which a large increase in strain occurs with little or no change in load, (5) a region called the strain hardening region in which the load again increases with increase in strain, but not as rapidly as in the elastic region, and (6) an unstable region past the ultimate load in which the load decreases with increasing strain. See Fig. 2 (adapted from reference 3) for a schematic representation of this stress-strain behavior. The phenomenon of strain hardening is explained in a variety of ways including the presence of imperfections, called dislocations, in the crystalline micro-structure. While dislocation theory provides a plausible explanation for much strain hardening and strain aging behavior, it will not be discussed further in this paper.

One strain hardening theory<sup>5</sup> states that  $\bar{\sigma}$  may be expressed as a function of  $\bar{\epsilon}$ , or

$$\bar{\sigma} = F(\bar{\epsilon}) \quad (6)$$

The equivalent stress  $\bar{\sigma}$  may be determined from the distortion energy yield criterion to be

$$\bar{\sigma} = \frac{1}{\sqrt{2}} \sqrt{(\sigma_1' - \sigma_2')^2 + (\sigma_2' - \sigma_3')^2 + (\sigma_3' - \sigma_1')^2} \quad (7)$$

where  $\sigma_1'$ ,  $\sigma_2'$ , and  $\sigma_3'$  are the principal stresses expressed in terms of true stress. The equivalent strain  $\bar{\epsilon}$  may be found from

$$\bar{\epsilon} = \frac{\sqrt{2}}{3} \sqrt{(\epsilon_1' - \epsilon_2')^2 + (\epsilon_2' - \epsilon_3')^2 + (\epsilon_3' - \epsilon_1')^2} \quad (8)$$

where  $\epsilon_1'$ ,  $\epsilon_2'$ , and  $\epsilon_3'$  are natural principal strains.

In Equation 6, F is a function depending on the characteristics of the metal involved. F may be found, for example, from the stress-strain curve of a simple tensile specimen, and is assumed valid for other states of stress subject to the following limitations: (1) The material is isotropic under plastic conditions. (2) Elastic strains are negligible in comparison with plastic strains. (3) Shearing stresses are responsible for plastic deformations, but normal stresses are not. (4) The ratios of the principal strains remain constant throughout the straining which takes place, i.e.  $\epsilon_2/\epsilon_1$  and  $\epsilon_3/\epsilon_1$  remain constant. (5) The principal axes of successive strain increments do not rotate with respect to the element. (6) The tensile and compressive stress-strain curves coincide when expressed in terms of true stress and true strain. (7) No Bauschinger effect is present. (8) There is no change in volume due to plastic deformation. The experimental and analytical results of the first investigation<sup>1</sup> showed the total error attributable to these assumptions to be reasonably small.

For many steels and some other metals, a plot of the logarithm of the effective stress versus the effective strain appears as a straight line. When this is true the inelastic portion of the stress-strain curve may be represented by the power function

$$\bar{\sigma} = k(\bar{\epsilon})^n \quad (9)$$

Examples of this type of stress-strain curve may be seen in Figs. 3-5.

Note that for the condition of uniaxial tension represented in these curves

$$\bar{\sigma} = \sigma_1' \text{ and } \bar{\epsilon} = \epsilon_1'$$

Reference 1 gave the following empirical equations for the strength coefficient and the strain hardening exponent:

$$k = 2.80 \sigma_u - 1.55 \sigma_y \quad (10)$$

and

$$n = 0.225 \sigma_u / \sigma_y - 0.120 \quad (11)$$

In remaining portions of this paper, values of the materials constants calculated by Equations 10 and 11 will be referred to as  $k_1$  and  $n_1$ .

**Strain Aging.** When a steel specimen is loaded in the plastic range, unloaded, and immediately reloaded, the yield strength of the mild steel is increased up to the point where the specimen was unloaded. This phenomenon is known as strain hardening. Now, if a time is allowed to pass after unloading, the yield strength of the specimen may be further increased, i.e. more than the increase due to strain hardening. This phenomenon is known as strain aging. It causes the yield plateau to be re-established, and causes increases in both the yield strength and in the ultimate strength. On the other hand, the ductility of the material is reduced, Fig. 2.

**Corner Model.** To analyze the cold-forming strains, a corner model was chosen<sup>1</sup> in which application of bending moment to a wide flat sheet produces a uniform curvature as shown in Fig. 6. If  $r_0$  is taken as the radius to the surface of zero strain, the engineering strain on a surface with a radius r is

$$\epsilon_\theta = r/r_0 - 1 \quad (12)$$

The corner model is assumed to be in a condition of plane strain. Consequently,  $\epsilon_z' = 0$ . For a constant volume condition, which is often assumed under conditions of plastic strain, the volume strain is zero. Hence,

$$\epsilon_r' = -\epsilon_\theta' \quad (13)$$

Substitution in Equation 8 results in

$$\bar{\epsilon} = \frac{2}{\sqrt{3}} \ln(r/r_0) \quad (14)$$

Assuming that Equation 9 is valid in compression as well as in tension, one may find the average corner yield strength  $\sigma_{yc}$  by integrating the effective stress over the full area of a corner:

$$\frac{\sigma_{yc}}{k} = \frac{r_0}{t} \int_1^{b/r_0} \left( \frac{2}{\sqrt{3}} \ln x \right)^n dx + \int_{a/r_0}^1 \left( \frac{2}{\sqrt{3}} \ln x \right)^n dx \quad (15)$$

where a and b are the inside and outside corner radii as shown in Fig. 6, and  $x = r/r_0$ . Equation 15 was evaluated numerically, assuming that the axis of zero strain to be located at  $r_0 = \sqrt{ab}$ , from  $a/t = 1$  to  $a/t = 10$ . These results were given in Reference 1. It was found that Equation 15 could be closely approximated by the formula

$$\sigma_{yc} = \frac{kb}{(a/t)^m} \quad (16)$$

where

$$b = 0.945 - 1.315 n \quad (17)$$

and

$$m = 0.803 n \quad (18)$$

Equation 15 was re-evaluated in this study for a/t ratios from 1 to 100. Fig. 7. It was found that Equation 15 could still be closely approximated by Equation 16. However, the extension of the lines in Figure 7 necessitated modification of the constants b and m. The revised equations for these constants were now found from Figs. 8 and 9 to be

$$b = 0.942 - 1.04 n \quad (19)$$

and

$$m = n \quad (20)$$

Equations 16, 19, and 20 will be utilized in a following section to predict three sets of corner yield strength values. To do this, the material constants  $k$  and  $n$  will be determined from: (1) Equations 10 and 11 ( $k_1$  and  $n_1$ ), (2) virgin tensile specimen test values ( $k_2$  and  $n_2$ ), and (3) prestrained and aged tensile specimen test values ( $k_3$  and  $n_3$ ).

#### EXPERIMENTAL INVESTIGATION

Tensile and compressive flat and corner test specimens were taken from a hot-rolled 16 gage sheet steel. The corner specimens were all formed by press braking. The inside radius of each corner specimen was measured by means of radius gages. The following paragraphs describe the test procedures and results.

Standard Tensile Tests of Virgin Sheet Steel. Six specimens were prepared from flat unworked sheet steel in accordance with ASTM standard dimensions given in Fig. 10(a). Tension tests were carried out using a microformer gage. The resulting tensile yield and ultimate strengths are given in the first half of Table I.

Tensile Tests for Inelastic Constants of Virgin Steel. Three tensile test specimens were made from flat unworked sheet steel in accordance with Fig. 10(a) as before. Two marks were made 2 in. apart on the specimens prior to their placement in the testing machine. Extensions in the plastic domain were measured by means of dividers and a steel rule, the load being noted at each extension of 0.05 in. When the testing was completed, values of true stress and true strain were computed and plotted on log-log paper, Figs. 3-5. In each plot, the strength coefficient  $k$  appears as the intercept of the  $\epsilon' = 1.0$  axis, and the strain hardening exponent  $n$  is the slope of the straight line.

Tensile Tests for Inelastic Constants from Prestrained and Aged Specimens. Five tensile specimens were made to the dimensions of Fig. 10(a). These specimens were loaded beyond the elastic limit the loads being noted at each predetermined elongation. Next, the specimens were artificially aged by placement for one-half hour in an oven preheated to 100°C. The specimens were then retested, elongations and loads being noted. The yield strengths were found by the 0.2% offset method and plotted as true yield stress versus true strain at prestrain, Fig. 11. Note the resulting straight line from which values of  $k$  and  $n$  were computed.

Tensile Tests of Cold-Formed Corners. Eighteen specimens were made in accordance with Figs. 10(b) and (c). These tensile tests were carried out using a microformer gage. Test results are given in Table II.

Compressive Tests. Six compressive specimens were prepared from the unworked flat sheet material in accordance with the dimensions shown in Fig. 10(d). Eighteen compressive specimens of three inch length were also cut from cold-formed corners. These specimens were greased, wrapped with aluminum foil, and then cast in hydrostone inside 3/4 in. diameter aluminum conduit cut to 3-13/16 in. lengths. This procedure was followed to prevent buckling in the specimens while measuring compressive loads and deformations. The compressive yield strengths for the six flat speci-

mens are given in Table I and those for the eighteen corner specimens in Table III.

Test Results. From Table I it may be seen that the average virgin yield strength is 46.9 ksi for tensile and 45.6 ksi for the compressive specimens. The average virgin tensile ultimate strength was 58.0 ksi.

The values for the inelastic materials constants  $k$  and  $n$  were established in three ways in this study: (1) by the approximate Equations 10 and 11 repeated from Reference 1, ( $k_1 = 89.4$  ksi and  $n_1 = 0.158$ ), (2) from log-log plots of true stress versus true strain in the plastic region of virgin flat sheet specimens, Figs. 3-5, (ave  $k_2 = 88.2$  ksi and ave  $n_2 = 0.164$ ), (3) from a log-log plot of true yield stress versus true pre-strain of prestrained and artificially aged specimens, Fig. 11, ( $k_3 = 89.5$  ksi and  $n_3 = 0.114$ ). Note that the values of  $k$  are comparatively close for all three methods. The value of  $n$  for the strain aged method is much smaller than for the virgin materials methods, for which the values of  $n$  are relatively close.

All three sets of constants were used in Equations 16, 19, and 20 in predicting corner yield strengths. The resulting curves are plotted as straight lines on the log-log plot of Fig. 12. The compressive and tensile yield strengths of corners are also shown on this figure. Curves 1 and 2 for constants  $k_1, n_1$  and  $k_2, n_2$ , compare well with the experimentally obtained corner yield strengths for  $a/t$  ratios up to 10, but not beyond. On the other hand, curve 3, corresponding to strain aged constants  $k_3, n_3$ , compares more favorably with the experimental corner yield strengths for the larger  $a/t$  ratios, but not for the smaller  $a/t$  ratios. It should also be noted that this third curve predicts all of the larger corner yield strengths slightly conservatively.

The maximum increase in corner yield strength was 47 percent for an  $a/t$  ratio of 1.38. The smallest increase in corner yield strength was 1 percent for an  $a/t$  ratio of 68.7. For  $a/t$  ratios greater than 30, the increase in corner yield strength results are comparatively small (i.e. in the range of 8 percent for an  $a/t$  ratio of 34 to 1 percent for an  $a/t$  ratio of 69, Tables II and III).

The stress-strain curves (not shown herein) for corners with small  $a/t$  ratios (large amounts of cold work) were gradual yielding, while those for corners with large  $a/t$  ratios (small amounts of cold work) were sharp yielding. The gradual yielding nature of stress-strain curves for corners with small  $a/t$  ratios may be explained as follows: The cold-forming strains in a small  $a/t$  ratio corner vary from zero at the surface of zero strain to greater than ultimate strain at the outside of the corner. Hence, when the corner is tested, the fibers near the surface of zero strain yield first and those near the outside and inside surfaces yield last. Furthermore, the tendency of strain aging to restore the yield plateau is not present in such highly deformed corners. On the other hand, in corners with large  $a/t$  ratios, the tendency for strain aging to restore the sharp yielding nature of the stress-strain diagram is present because the degree of cold work is not large.<sup>3</sup>

New empirical equations for the constants  $b$  and  $m$  have been established from Figs. 8 and 9. These curves indicate that the extension of  $a/t$  ratios up to 100 reduces the slope of the plots compared with previously established<sup>1</sup> results for  $a/t$  ratios up to 10.

TABLE I  
YIELD AND ULTIMATE STRENGTHS OF  
VIRGIN SHEET STEEL

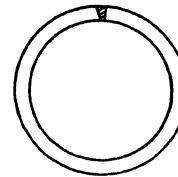
Specimen	Type	Yield Strength (ksi)	Ultimate Strength (ksi)
1	Tensile	40.8	56.3
2		47.6	58.8
3		48.0	57.9
4		48.6	58.5
5		48.6	58.4
6		47.8	58.3
Average	Tensile	46.9	58.0
1	Compressive	45.8	----
2		49.6	----
3		42.5	----
4		44.6	----
5		51.7	----
6		39.5	----
Average	Compressive	45.6	

TABLE II  
CORNER TENSILE YIELD AND  
ULTIMATE STRENGTH VALUES

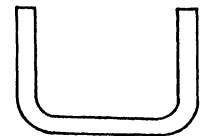
Speciman	a/t Ratio	Yield Strength $\sigma_{yc}$ (ksi)	Ultimate Strength $\sigma_u$	$\frac{\sigma_{yc}}{\sigma_y \text{ tens.}}$
1	1.918	63.1	68.4	1.34
2	1.667	66.9	74.6	1.42
3	1.892	60.4	63.9	1.29
4	1.410	64.8	72.1	1.38
5	1.423	63.9	67.7	1.36
6	1.157	64.0	76.2	1.36
7	5.109	58.3	62.8	1.24
8	5.236	57.0	60.7	1.22
9	5.154	53.7	61.8	1.14
10	8.547	50.2	61.1	1.07
11	8.635	49.3	60.1	1.05
12	8.508	53.1	62.4	1.13
13	70.8	48.0	57.7	1.02
14	44.6	49.7	58.2	1.06
15	67.3	48.5	57.5	1.03
16	34.7	49.0	57.8	1.04
17	36.5	48.0	57.3	1.02
18	35.7	48.5	58.2	1.03

TABLE III  
CORNER COMPRESSIVE  
YIELD STRENGTH VALUES

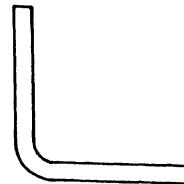
Specimen	Ratio	Yield Strength $\sigma_{yc}$ (ksi)	$\frac{\sigma_{yc}}{\sigma_y \text{ compr.}}$
1	1.624	62.8	1.38
2	2.181	62.2	1.36
3	1.644	65.6	1.44
4	1.373	66.0	1.45
5	1.382	66.8	1.47
6	1.361	63.9	1.40
7	33.44	49.6	1.09
8	35.11	49.5	1.09
9	33.78	49.1	1.08
10	68.73	45.9	1.01
11	65.18	45.7	1.01
12	65.18	45.7	1.01
13	5.208	51.1	1.12
14	5.163	52.9	1.16
15	5.630	52.1	1.14
16	8.591	49.2	1.08
17	8.881	49.5	1.09
18	8.741	48.6	1.07



WELDED PIPE



CHANNEL SECTION



ANGLE SECTION

FIG. 1. COMMON COLD-FORMED LIGHT GAGE STEEL SECTIONS

- A virgin curve
- B unloading in strain hardening range
- C immediate reloading
- D reloading after strain aging

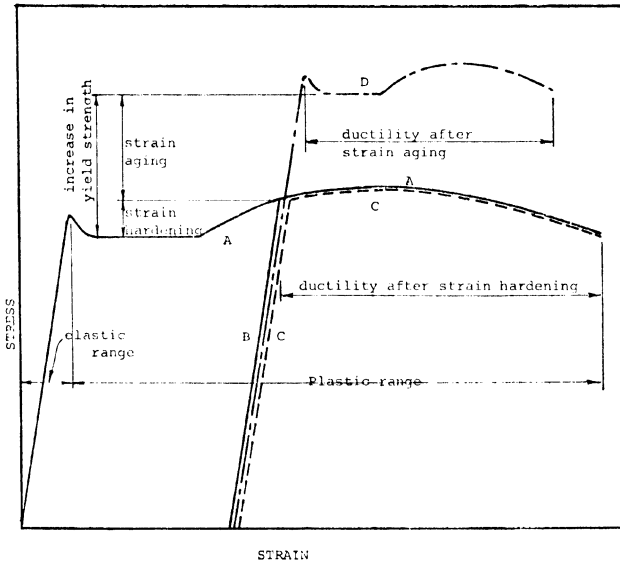


FIG. 2. STRESS-STRAIN CHARACTERISTICS OF MILD STEEL WITH DIFFERENT LOADING HISTORIES.

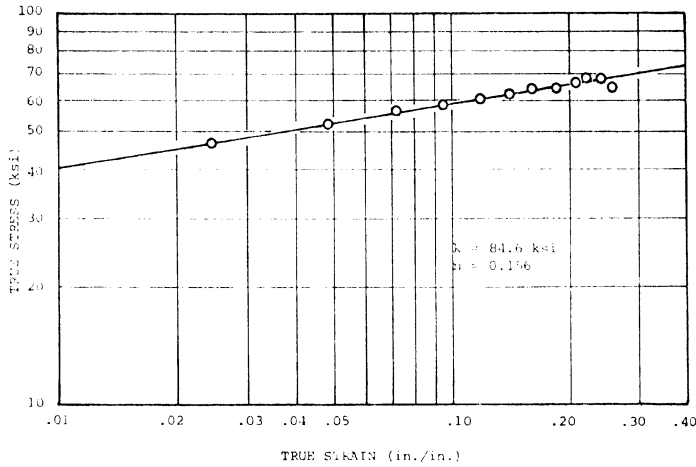


FIG. 4. TENSILE STRESS-STRAIN CURVE FOR VIRGIN MATERIAL SPECIMEN P2 IN TERMS OF TRUE STRESS AND TRUE STRAIN.

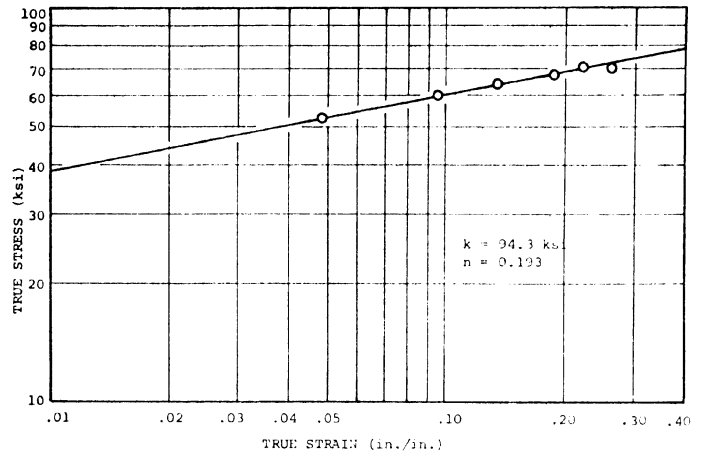


FIG. 3. TENSILE STRESS-STRAIN CURVE FOR VIRGIN MATERIAL SPECIMEN P1 IN TERMS OF TRUE STRESS AND TRUE STRAIN.

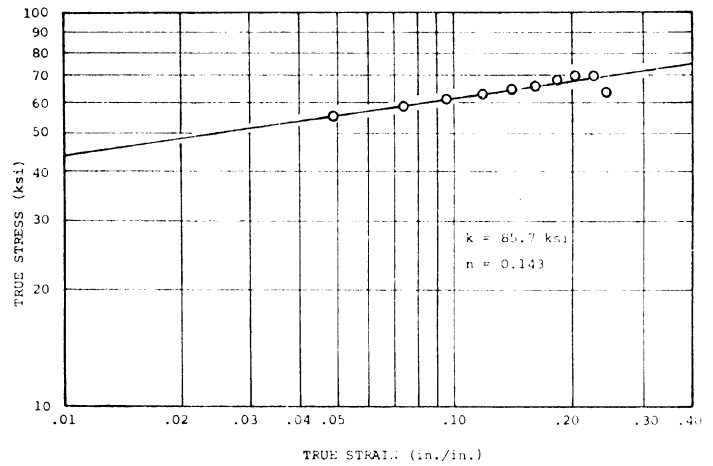


FIG. 5. TENSILE STRESS-STRAIN CURVE FOR VIRGIN MATERIAL SPECIMEN P3 IN TERMS OF TRUE STRESS AND TRUE STRAIN.

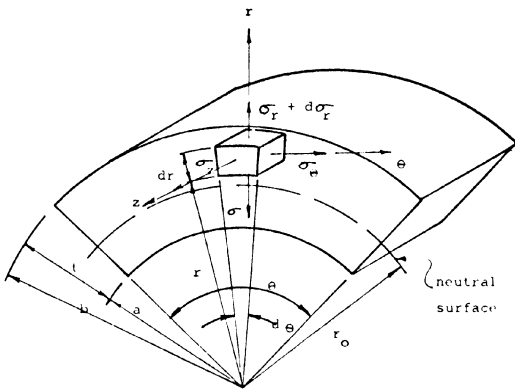


FIG. 6. STRESSES ON VOLUME ELEMENT OF PLASTICALLY DEFORMED PLATE.

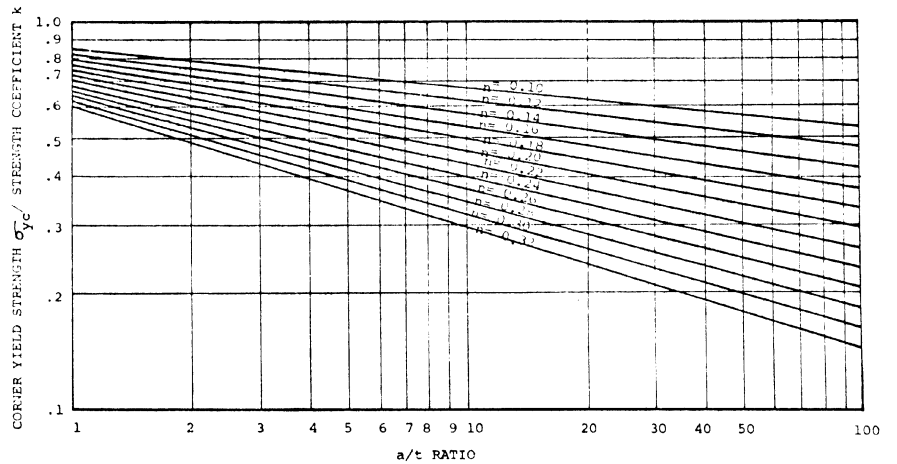


FIG. 7. CORNER YIELD STRENGTH AS A FUNCTION OF  $b$ ,  $k$ ,  $m$ ,  $n$ , and  $a/t$ .

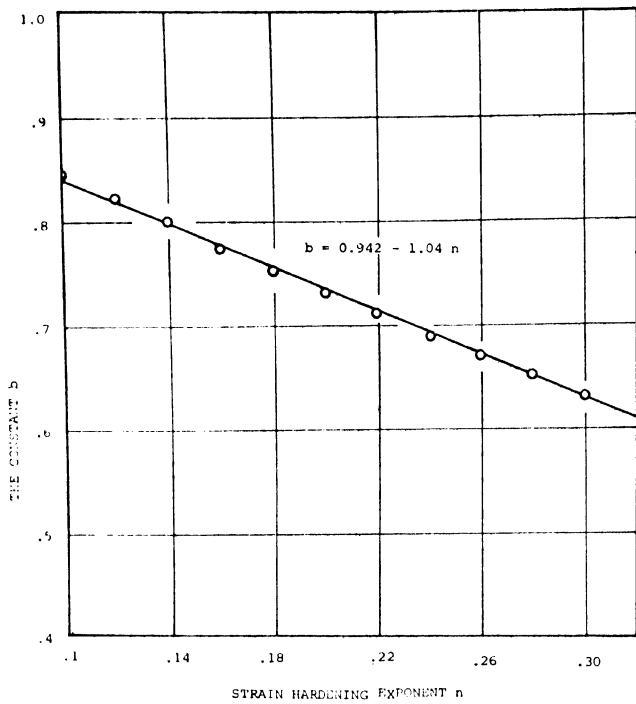


FIG. 8. THE CONSTANT  $b$  AS A FUNCTION OF THE STRAIN HARDENING EXPONENT.

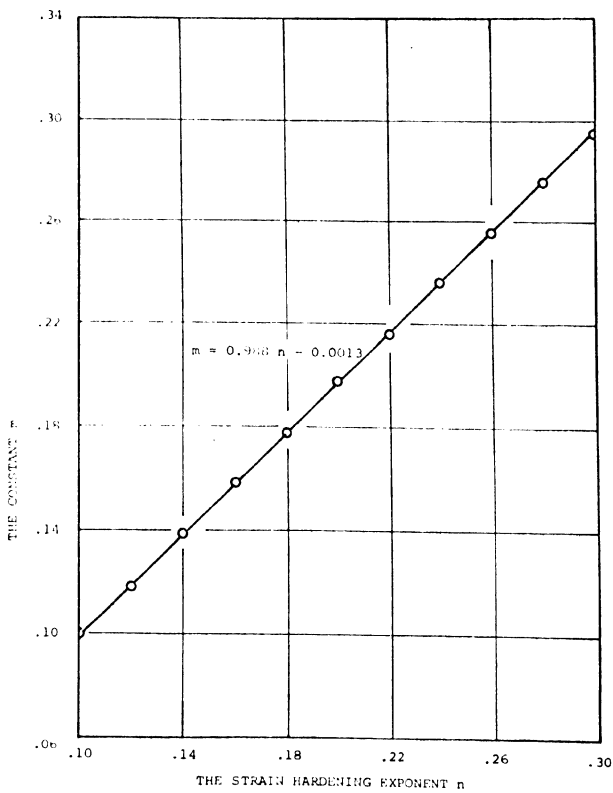


FIG. 9. THE CONSTANT  $m$  AS A FUNCTION OF THE STRAIN HARDENING EXPONENT.

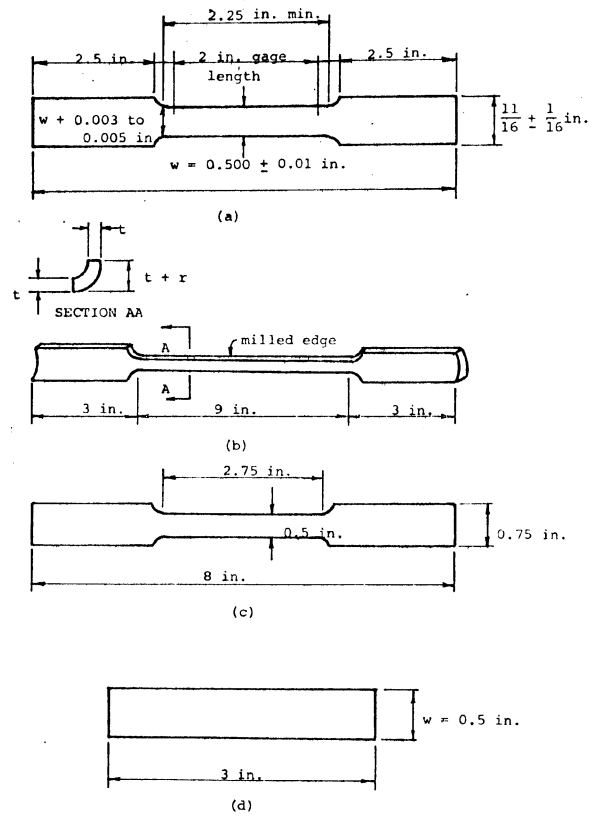


FIG. 10. TYPICAL SPECIMENS. (a) STANDARD ASTM FLAT STEEL SPECIMEN. (b) TENSILE CORNER SPECIMEN WITH INSIDE RADIUS  $a$  NOT LARGER THAN 0.5 INCH. (c) TENSILE CORNER SPECIMEN WITH INSIDE RADIUS  $a$  LARGER THAN 0.5 INCH. (d) COMPRESSIVE FLAT SPECIMEN.

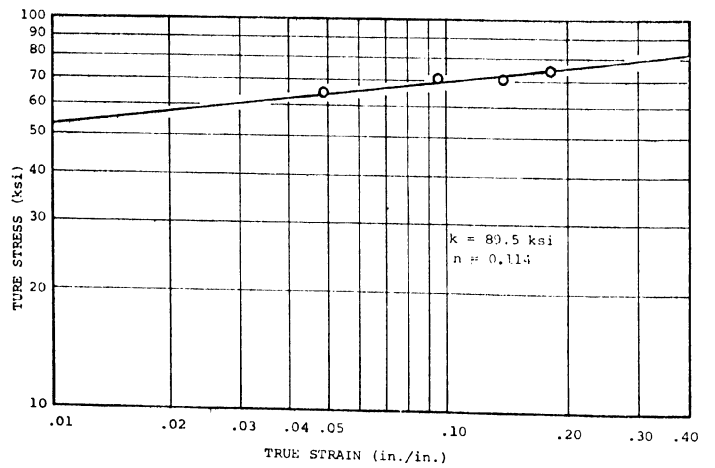


FIG. 11. TENSILE STRESS-STRAIN CURVE FOR STRAIN AGED SPECIMENS IN TERMS OF TRUE STRESS AND TRUE STRAIN.

Curve 1:  $k_1$  and  $n_1$  based on Eqs. 10 and 11 from Reference 1.  
 Curve 2:  $k_2$  and  $n_2$  based on average values from virgin tensile specimens, Figs. 3-5.  
 Curve 3:  $k_3$  and  $n_3$  based on values from prestrained and aged specimens, Fig. 11.

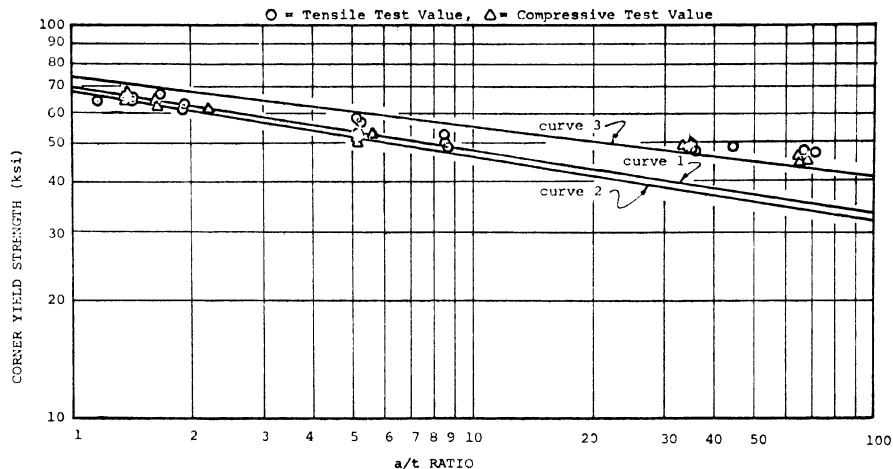


FIG. 12. EXPERIMENTAL AND ANALYTICAL CORNER YIELD STRENGTH VALUES COMPARED.

LIST OF REFERENCES

1. Karren, Kenneth W., "Corner Properties of Cold-Formed Steel Shapes," *Journal of the Structural Division A.S.C.E.* Vol. 93, No. ST1, February, 1967, pp. 401 to 432.
2. Kuper, E. J. and Macadam, J. N., "Quantitative Effects of Strain Hardening on the Mechanical Properties of Cold-Formed Electric Welded Steel Tubing", Presented at the A.I.M.E. Operating Metallurgy Conference, December 13, 1967.
3. Chajes, Alexander; Britvec, S. J.; and Winter, George, "Effect of Cold-Straining on Structural Steels", *Journal of the Structural Division, A.S.C.E.*, Vol. 89, No. ST 2, Proc. Paper 3477, April, 1963, pp. 1-32.
4. Gohil, M. M., "The Yield Strength of Light-Gage Cold-Formed Steel Corners", Unpublished M.S. Thesis, Brigham Young University, May, 1968.
5. Hill, R., *The Mathematical Theory of Plasticity*, Oxford University Press, London, 1950.
6. Richards, Cedric W., *Engineering Materials Science*, Wardsworth Publishing Co., Inc., Belmont, California, 1961, pp. 77-86 and 95-97.

SUMMARY AND CONCLUSIONS

1. The experimental results of this investigation show that cold-forming increases the yield strength of corners, the variation of increase being

1% for an a/t ratio of 69 to 4% for an a/t ratio of 1.38. The percentage increase in ultimate strength was not as large, being a maximum of 29% for an a/t ratio of 1.67.

2. The analytical technique of a previous investigation<sup>1</sup> for predicting corner yield strengths has been successfully extended to a/t ratios above 10 for a hot rolled light-gage sheet steel material. The relation  $\sigma_{yc} = kb/(a/t)^m$  (Equation 16) holds good for such larger a/t ratios providing one includes the influence of strain aging. The equations for b and m (Equations 19 and 20) have been revised somewhat from those of the previous investigation (Equations 17 and 18).

3. The influence of strain aging on the increase in yield strength is negligible for small values of a/t, but becomes significant for large values of a/t.

4. Strain aging seems to decrease the value of the strain hardening exponent n. This may be due to a decrease in ductility and lesser margin of difference between the yield strength and the ultimate strength after strain aging.

RECOMMENDATIONS FOR FURTHER STUDY

1. Since this investigation was not funded, the testing was limited to one type of material. To further check the validity of the method, similar tests should be conducted on several types of material.